Variation in the structural and magnetic properties induced by La doping in $Pr(Br_{1-x}La_x)_2Cu_3O_{7+y}$

H. Y. Wang, C. H. Chang, S. R. Hwang, W.-H. Li, and K. C. Lee
Department of Physics, National Central University, Chung-Li, Taiwan 32054, Republic of China

J. W. Lynn
NIST Center for Neutron Research, NIST, Gaithersburg, Maryland 20899

H. M. Luo and H. C. Ku
Department of Physics, National Tsing-Hua University, Hsinchu, Taiwan 300, Republic of China
(Received 24 May 2000)

Neutron diffraction and ac magnetic susceptibility measurements were performed to study the effects of La doping on the structural and magnetic properties of polycrystalline $Pr(Ba_{1-x}La_x)_2Cu_3O_{7+y}$. Structural studies using high-resolution neutron diffraction and Rietveld analysis indicate that La doping triggers the occupation of O on the antichain sites which reduces the degree of orthorhombicity in the system. Tetragonal symmetry was observed in the 29% La-doped compound. Magnetic orderings of the Pr ions as well as the Cu ions were evident in the susceptibility. The Pr spin ordering was confirmed by the neutron magnetic diffraction data. Significant reductions in the ordering temperature of Pr were found upon increased La doping, while the spin configuration remained. No obvious changes were observed in the ordering temperature of Cu.

I. INTRODUCTION

Among the superconducting oxides $RBa_2Cu_3O_{7-y}$ ($R123$, R=rare earth), the unique electronic and magnetic properties of the R=Pr compound have triggered intense study over the past decade. Currently, the hybridization between the Pr-4f orbital and the neighboring O-2p_π orbital in the CuO_2 layers is believed to be the most significant mechanism governing[1–4] the general behavior of Pr123. Still, the mechanisms for the absence of superconductivity[5–7] and the high antiferromagnetic ordering temperature (T_N=17 K) of the Pr spins[8–10] remain puzzling. Recently, observations[11,12] of inhomogeneous superconductivity in Pr123 have been reported. Arguments for the appearance of superconductivity have pointed in the direction that Pr ions are incorporated into the Ba sites and that the O sites are fully occupied. Apparently, BaO layers may also play an important role affecting the general properties of the systems. The addition of excess R into the Ba sites often results in oxygen defects on the antichain sites.[13–18] A complex structural change has been observed[17] in $Nd_{1+x}Ba_{2-x}Cu_3O_{7+y}$, where excess Nd was introduced into the Ba sites. Superconductivity was also found[18] to be depressed when Pr was introduced into the Ba sites in systems such as $Nd(Ba_{1-x}Pr_x)_2Cu_3O_{7+y}$. A 50% replacement of the Ba by Sr in $TlBa_2PrCu_2O_7$ significantly alters the ground-state spin structure of the Cu ions,[19] demonstrating that the BaO layers also actively participate in the coupling between the Cu spins.

In this paper, we report results from studies made on the crystal structure and the magnetic properties of a series of four polycrystalline $Pr(Ba_{1-x}La_x)_2Cu_3O_{7+y}$, where nonmagnetic La ions were incorporated into the Ba sites, using ac magnetic susceptibility and neutron-diffraction measurements. We concentrated on the effects resulting from La being incorporated into the Ba sites, on the crystal symmetry, on the Pr spin ordering, and on the Cu spin ordering. As divalent Ba was partially replaced by trivalent La, excess O entered the antichain sites, resulting in a structural change from an orthorhombic $Pmmm$ symmetry to a tetragonal $P4/mmm$ symmetry. The T_N of Pr was significantly reduced, while the spin structure remained. No obvious changes of the Cu spin ordering were observed.

II. EXPERIMENTAL DETAILS

Four oxygenated La-doped Pr123 polycrystalline samples having nominal compositions $Pr(Ba_{1-x}La_x)_2Cu_3O_{7+y}$, with x=0.1, 0.15, 0.2, and 0.3, were prepared by the standard solid-state reaction technique. For each compound, high-purity $BaCO_3$, Pr_6O_{11}, La_2O_3, and CuO powders were well mixed in stoichiometric ratios, and then calcined in floating Ar gas at 940 °C for 24 h, using a heating rate of 300 °C/h. The calcined powder was pressed into pellets and sintered in floating Ar gas, to avoid the formation of magnetic $PrBaO_3$, at 900 °C for 24 h, followed by cooling to room temperature at a cooling rate of 60 °C/h. The resultant powder was oxygenated by annealing in floating O_2 gas at 400 °C for 24 h, and then naturally furnace cooled to room temperature. X-ray-diffraction measurements were then used to characterize the samples, pellet by pellet. No obvious difference was found in the diffraction patterns taken from different portions of the sample.

Crystal structures of the compounds were determined by complete structural analysis using high-resolution neutron-diffraction measurements and the Rietveld refinement method.[20] These measurements were performed on BT-1,. the 32-detector powder diffractometer at the NIST Center for Neutron Research. For these measurements, the samples

were loaded into cylindrical vanadium cans, which produced no measurable neutron diffraction peaks. A Cu(311) monochromator crystal was used to select a wavelength of $\lambda = 1.5401$ Å for the incident neutrons. Angular collimators with horizontal divergences of 15′, 20′, and 7′ full width at half maximum (FWHM) acceptance were employed for the in-pile, monochromatic, and diffracted beams, respectively.

The effects of La doping on the magnetic ordering of the Pr and Cu ions were studied by measuring the ac magnetic susceptibility and the magnetic neutron-diffraction patterns. The ac susceptibilities were measured on a conventional ac susceptometer, where the sample was subjected to a weak driving ac magnetic field and the response of the system was detected using two identical sensing coils connected in opposition. For these measurements, samples were loaded into cylindrical plastic containers, and a pumped ^{4}He cryostat, operated between 1.8 and 400 K, was used to control the sample temperature. Magnetic neutron-diffraction experiments were also conducted at NIST using the BT-2 triple-axis spectrometer, operated in double-axis mode. A pyrolytic graphite PG(002) monochromator was employed to select neutrons of $\lambda = 2.359$ Å, and a PG filter was placed after the monochromator position to suppress high-order wavelength contamination. Angular collimators used had 60′, 40′, and 40′ FWHM acceptance. For these measurements, samples were loaded into cylindrical aluminum cans filled with helium exchange gas to facilitate thermal conduction, and the sample temperature was controlled using a pumped ^{4}He cryostat, operated between 1.4 and 25 K.

III. RESULTS AND DISCUSSION

High-resolution neutron-diffraction patterns, covering a scattering-angle range from 3° to 168°, taken at room temperature were first collected to characterize the samples and determine the detailed structural parameters. Temperature dependences of the ac susceptibility, performed using various driving fields, were then measured to study the basic magnetic response of the system and to search for magnetic anomalies. Both the in-phase component, $\chi'(T)$, and the out-of-phase component, $\chi''(T)$, were measured simultaneously. Neutron-diffraction patterns covering certain temperature regimes, where the susceptibility showed anomalies, were then collected to search for magnetic signals. As no structural change was observed within the temperature regime studied, the magnetic signals were isolated from the nuclear ones by employing the standard subtraction technique,[21] where the diffraction pattern taken at a temperature well above the ordering temperature was subtracted from the one taken well below. The uncertainties quoted throughout this paper are statistical and represent one standard deviation.

A. Structural change

Structural analysis[22] has shown that fully oxygenated Y123 crystallizes into an orthorhombic *Pmmm* symmetry. This orthorhombicity is caused by the formation of CuO-chain layers (*a*-*b* planes), in which there are O ions between the Cu ions (forming Cu-O chains) along only one crystallographic axis (the *b* axis). It is generally said that the O ions in the CuO-chain layers occupy the chain sites (the sites between the Cu ions along the *b* axis) while leaving the antichain sites (the sites between the Cu ions along the *a* axis) vacant. Using trivalent La ions to partially replace divalent Ba ions may tend to pull more O atoms into the system, thus compensating for the additional charges arriving from the La^{3+}. O occupation on the antichain sites and a change of crystalline structure into a *P*4/*mmm* symmetry may then be anticipated for the La-doped systems.

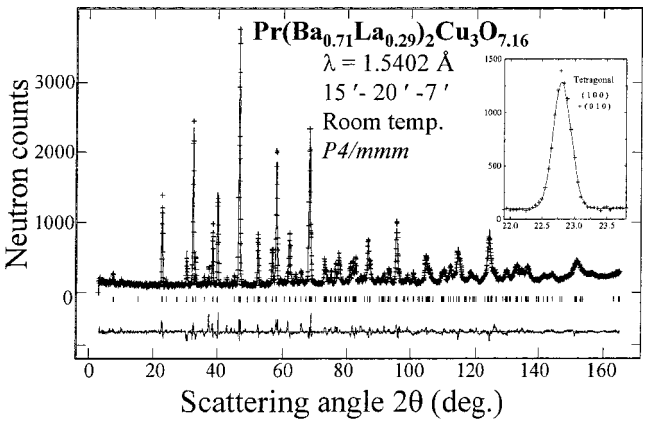

FIG. 1. Observed (crosses) and fitted (solid lines) high-resolution neutron power-diffraction patterns collected at room temperature. The short vertical lines shown below the pattern mark the calculated positions of Bragg reflections for the proposed structure.

The diffraction patterns were analyzed using the GSAS (general structure analysis system) program,[23] following the Rietveld refinement method. Several models with different symmetries were assumed during the preliminary analysis, with special concentration on the expected[18] *Pmmm* and *P*4/*mmm* symmetries. All the structural and lattice parameters were allowed to vary simultaneously, and refining processes were carried out until R_W, the weighted R factor, differed by less than one part in 1,000 within two successive cycles. The $x = 0.1$, 0.15, and 0.2 compounds crystallized into an orthorhombic symmetry of the space group *Pmm*, whereas the $x = 0.3$ compound crystallized into a tetragonal symmetry of the space group *P*4/*mmm*. No mixing of the two structural phases was found in all four compounds. Figure 1 shows the observed (crosses) and fitted (solid lines) patterns for the $x = 0.3$ compound, with their differences plotted at the bottom indicating they agree very well. In the inset to Fig. 1, the (100)+(010) peak is plotted in an expanded scale, showing that the (100) peak coincided with the (010) peak for tetragonal symmetry. The refined structural parameters and the selected bond lengths for all four compounds are listed in Table I, where the center of the unit cell is defined as at the Pr site.

Refinements that allowed La to enter the Pr sites gave an unacceptable negative occupancy factor for La, indicating that no La atoms occupied the Pr sites. Poorer fits resulted when Pr was allowed to enter the Ba sites or Ba to enter the Pr sites, showing that La doping did not alter the periodicity of the Pr ions. We note, however, that the neutron-scattering amplitudes for Pr and Ba differed by only 10%, which reduces its ability to resolve Pr from Ba by neutrons. The chemical formulas for the four compounds, obtained from the structural analysis, are $Pr(Ba_{0.91}La_{0.09})_2Cu_3O_{7.06}$, $Pr(Ba_{0.86}La_{0.14})_2Cu_3O_{7.12}$, $Pr(Ba_{0.72}La_{0.18})_2Cu_3O_{7.14}$, and

TABLE I. Refined structural parameters for $Pr(Ba_{1x}La_x)_2Cu_3O_{7+y}$, where B represents the isotropic temperature parameter. The center of the unit cell is defined as at the Pr site, so that Pr($\frac{1}{2}\frac{1}{2}\frac{1}{2}$), Ba/La($\frac{1}{2}\frac{1}{2}z$), O(1)($xyz$), Cu(2)(00$z$), O(2)($\frac{1}{2}0z$), O(3)($0\frac{1}{2}z$), Cu(1)(000), O(4)($x\frac{1}{2}0$), and O(5)($\frac{1}{2}y0$) show the orthorhombic symmetry. Setting O(2) and O(3) to be equivalent as well as O(4) and O(5) to be equivalent then reduce it to the tetragonal symmetry.

	$x=0.09(1)$	$x=0.14(1)$	$x=0.18(2)$	$x=0.29(1)$
Space group	*Pmmm*	*Pmmm*	*Pmmm*	*P*/4*mmm*
a (Å)	3.8844(2)	3.8908(5)	3.8964(4)	3.8922(1)
b (Å)	3.9077(2)	3.9027(4)	3.8981(3)	3.8922(1)
C (Å)	11.6879(4)	11.684(4)	11.6731(7)	11.6210(6)
Vol. (Å^3)	177.594	177.417	177.298	176.049
Pr B (Å^2)	0.13(7)	0.37(3)	0.18(1)	0.40(3)
Ba/La z	0.1799(2)	0.1791(3)	0.1801(3)	0.1772(4)
B (Å^2)	1.23(4)	0.98(2)	1.38(7)	1.26(3)
O(1) x	0.0383(2)	0.0412(2)	0.0450(5)	0.0635(7)
y	0.0339(2)	0.0426(1)	0.0590(4)	0.0635(7)
z	0.1588(2)	0.1586(2)	0.1572(4)	0.1591(4)
B (Å^2)	0.92(1)	0.40(1)	1.28(1)	0.74(1)
Cu(2) z	0.3500(2)	0.3502(6)	0.3504(2)	0.3491(2)
B (Å^2)	0.69(5)	1.27(5)	0.92(5)	1.37(3)
O(2) z	0.3696(2)	0.3696(5)	0.3694(4)	0.3695(2)
B (Å^2)	1.05(5)	1.61(1)	0.81(1)	1.25(4)
O(3) z	0.3726(3)	0.3713(5)	0.3701(4)	
B (Å^2)	0.66(1)	0.77(1)	0.98(1)	
Cu(1) B (Å^2)	1.14(7)	1.16(5)	1.16(4)	1.46(7)
O(4) x	0.0529(2)	0.0601(4)	0.0663(3)	
B (Å^2)	1.46(3)	1.38(3)	1.35(4)	1.52(5)
O(5) y	0.0212(2)	0.0282(5)	0.0500(4)	
B (Å^2)	0.92(7)	1.43(5)	0.77(7)	
O(4) frac	0.4393(9)	0.4473(6)	0.4641(9)	0.5765(8)
O(5) frac	0.1840(1)	0.2204(8)	0.2200(9)	
O content	7.06(1)	7.12(1)	7.14(1)	7.16(1)
Pr-O(2)	2.4780(5) Å	2.4758(3) Å	2.4744(3) Å	2.46699(6) Å
Pr-O(3)	2.4492(5) Å	2.4591(3) Å	2.4686(4) Å	
χ	1.1112	1.479	1.686	2.172

$Pr(Ba_{0.31}La_{0.29})_2Cu_3O_{7.16}$, which correspond to the 9%, 14%, 18%, and 29% La-doped systems, respectively. They agree well with the stoichiometric compositions. In addition, structural analysis was also directed at searching for impurity phases such as $PrBaO_3$, $PrCuO_3$, $BaCuO_3$, and CuO_2. No traces of them were found, showing the samples to be essentially single phase. We estimated any impurity phases in the samples to be less than 2%.

Several features were seen and interpreted as divalent Ba atoms were partially replaced by trivalent La atoms: (1) La atoms entered the Ba sites, and no traces of La were found on the Pr sites. (2) No atoms other than Pr were found on the rare-earth sites, while Pr occupies its normal site, forming a simple Pr unit cell, as in an undoped system. (3) The O content progressively increases as the La concentration is increased. This intake of extra O onto the antichain sites will, we believe, compensate for the additional charges arriving due to the replacement of Ba^{2+} using La^{2+}, as expected. (4) Similar to what has been observed in isostructural Nd-doped[18] and Pr-doped[24] systems, the c axis is shortened by nearly 1% from the undoped to the 29% La-doped compounds. This is consistent with smaller La atoms being used to replace larger Ba atoms. However, the average separation between the Pr atoms and their neighboring O atoms increased. An 8.5% increase of the Pr-O(3) bond length was obtained, accompanied by a 3.3% decrease in the Pr-O(2) bond length. A similar qualitative behavior was also observed[18] in the isostructural Nd-doped system. This behavior is a direct consequence of the appearance of extra O atoms in the CuO_{1+y} layers, which pulls the neighboring (Ba/La)O and CuO_2 layers toward the CuO_{1+y} layers resulting in an increase in the separation between the Pr and CuO_2 layers. (5) The O(1) atoms in the (Ba/La)O layers shifted away from their normal positions, at the edges of the unit cell, by an amount related to the doping level. Figures 2(a) and 2(b) show the nuclear density contours of the (Ba/La)O layer viewed along the c axis for the 9 and 29% La-doped compounds, respectively. Both maps cover 7.78 Å$\times$7.78 Å, and the contours cover nuclear densities from 4.0 to 0.02 Å^{-3}. A fourfold symmetry was clearly seen for the contours representing the density of O(1), indicating that there are four O(1) which contribute to these contours. As listed in

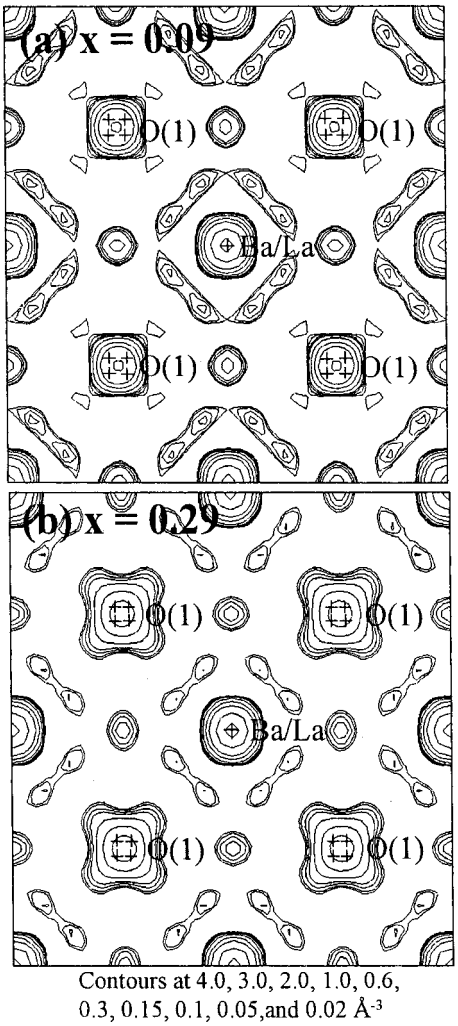

FIG. 2. Nuclear density maps of the (Ba/La)O layer viewed along the *c* axis for the (a) 9% and (b) 29% doped compounds. For densities of O(1), the contours display a fourfold symmetry.

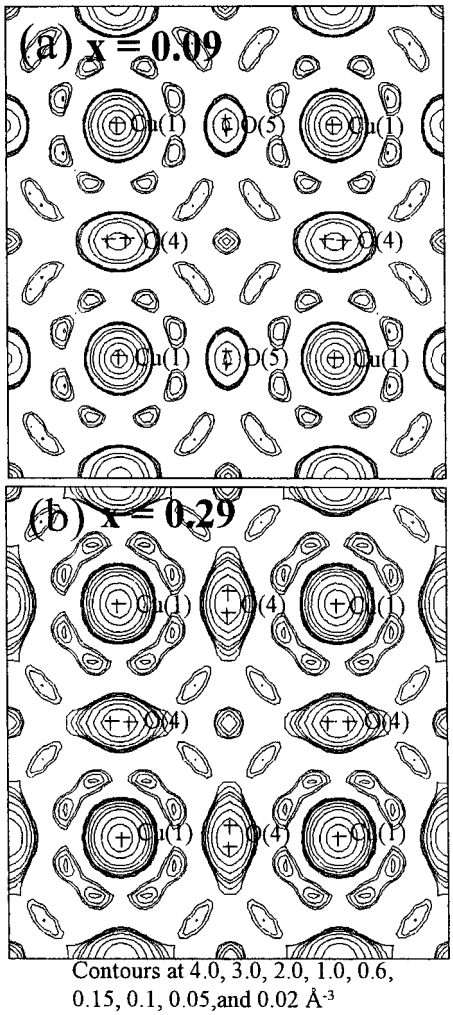

FIG. 3. Nuclear density maps of the CuO_{1+y} layer viewed along the *c* axis for the (a) 9% and (b) 29% doped compounds. The contours shown in (a) display a twofold symmetry, whereas a fourfold symmetry is seen for those shown in (b).

Table I a $\sim$ 6% shift along both the *a* and *b* axes was obtained for the 29%-doped compound. This shift, we believe, will help balance the appearance of two different atoms, La and Ba, in these layers. Note that refinements performed that allowed no shift in the O(1) gave an unacceptably large thermal factor for O(1), which in terms indicates the existence of the shift. (6) The occupation of antichain sites by O atoms reduces the degree of orthorhombicity of the unit cell. Unequal filling of the chain and antichain sites would preserve an orthorhombic symmetry, as observed for the 9, 14, and 18 % doped systems. The tetragonal symmetry observed for the 29% doped compound indicates that the chain and antichain sites are equally occupied. This orthorhombic-to-tetragonal structural change can be clearly seen in the nuclear density maps of the CuO-chain layers, viewed along the *c* axis, shown in Figs. 3(a) and 3(b), for the 9 and 29 % doped compounds, respectively. Clearly, the contours presented in Fig. 3(a) show a twofold symmetry whereas a fourfold symmetry is seen in those shown in Fig. 3(b).

B. Pr spin ordering

It is well known that the Pr spins in the undoped system order at $T_N = 17\,\mathrm{K}$, with a simple antiferromagnetic arrangement and a saturated moment of $0.74\mu_B$.[6,8,10] Shown in Figs. 4(a), 4(b), and 4(c) are the $\chi'(T)$, measured using a weak driving field with an rms strength of 1 Oe and a frequency of 100 Hz for the 9, 18, and 29 % doped compounds, respectively. The $\chi'(T)$ observed for the La-doped compounds are very similar to the one observed for the undoped system.[25–27] The solid curves shown in Fig. 4 indicate the fits of the data obtained between $25\,\mathrm{K} < T < 200\,\mathrm{K}$ to the Curie-Weiss expression for antiferromagnetic systems. No obvious changes in the effective moment were observed but a value of $\mu_{\mathrm{eff}}(\mathrm{Pr}) \approx 2.72(5)\mu_B$ was obtained for all three compounds. This value of $\mu_{\mathrm{eff}}(\mathrm{Pr})$ obtained for the La-doped compound was essentially the same value obtained for the undoped system.[6,25,26]

At low temperatures the data clearly departed from the fitted Curie-Weiss curves which signified the ordering of the Pr spins, as was observed in the undoped system.[6,25] The anomalies occurred at 13, 10, and 7 K for the 9, 18, and 29 % doped compounds, respectively, showing that La doping causes the Pr spins to order at a lower temperature. Generally, it is believed that the superexchange couplings between the Pr spins, mediated through the neighboring O atoms, are

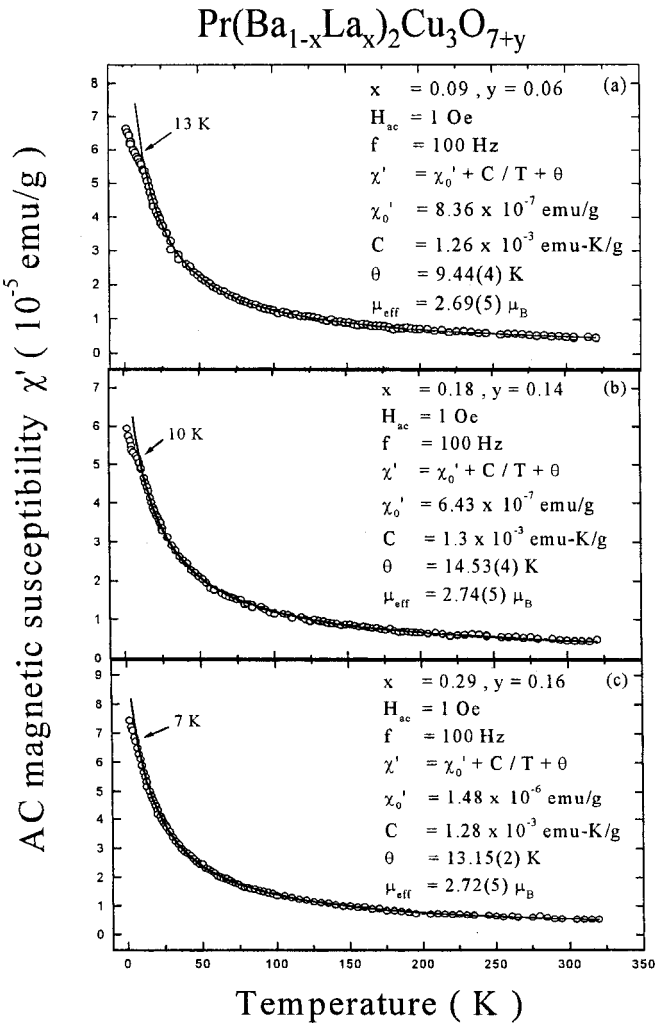

FIG. 4. Temperature dependence of the in-phase component of the ac susceptibility measured using a weak driving field with an rms strength of 1 Oe and a frequency of 100 Hz for (a) 9%, (b) 18%, and (c) 29% La-doped compounds. The inflection point, signifies the Pr ordering, shifts to a lower temperature as the La concentration is increased.

the main mechanism governing the Pr magnetism.[6,28,29] Direct hybridization between the Pr-4f and O-2p_π orbitals has been observed[30] in a charge density study using synchrotron radiation. Certainly, the strength of the coupling depends strongly on the separation between the Pr and the O atoms. The structural analysis shown above indicates that the La doping has resulted in an increase in the separation between the Pr ions and their neighboring O ions. A weaker coupling and a lower ordering temperature for the Pr spins may then be anticipated. In addition, below the ordering temperature, χ' increases as the temperature is further reduced. This behavior is similar to that is usually observed in other Pr containing high-T_c oxides, where the cusp in $\chi'(T)$ anticipated for antiferromagnetic system is not seen. No obvious differences were seen for $\chi'(T)$ measured with an applied dc magnetic field up to 1 T. No ac losses were detected, as essentially zero values were obtained for χ'' at all the temperatures studied.

The magnetic peaks that characterize the Pr ordering for the 29% La-doped compound are shown in the inset to Fig. 5, where the indices shown are based on the nuclear unit cell. This magnetic pattern was obtained by subtracting the pattern taken at 18 K from the one taken at 1.4 K, and signifies a simple antiferromagnetic structure for the Pr spins, as shown to the right in Fig. 5. This proposed magnetic structure and the relative intensities observed for the Pr in this La-doped compound are the same ones as have been observed[8] in the undoped system, showing that La doping does not alter the spin arrangement and saturated moment of the Pr ions. The temperature dependences of the peak intensities at the $\{\frac{1}{2}\frac{1}{2}\frac{1}{2}\}$ position for the 29 and 18% doped compounds are shown in Figs. 5 and 6, respectively, where the solid curves are only guides for the eye. These plots show variations of the square of the magnetization with temperature, and reveal typical order-parameter curves for polycrystalline samples. The ordering temperatures of the Pr spins, as determined by the inflection points of the order-parameter curves, for the 29 and 18% doped compounds, are $T_N \approx 10$ and 7 K, respectively, which match the temperatures at which $\chi'(T)$ show anomalies.

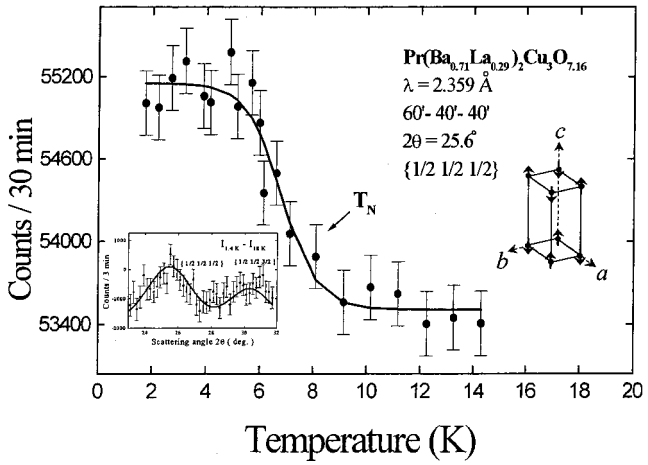

FIG. 5. Magnetic diffraction pattern obtained at 1.4 K, variation of the $\{\frac{1}{2}\frac{1}{2}\frac{1}{2}\}$ peak intensity with temperature, and the proposed magnetic structure for the Pr spins of the 29% La-doped compound. The solid curves shown in the magnetic diffraction pattern indicate the fits of the data to the Gaussian instrumental resolution functions.

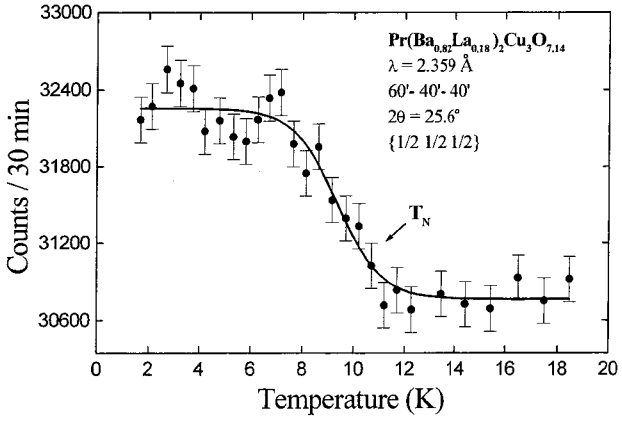

FIG. 6. Temperature dependence of the peak intensity at the $\{\frac{1}{2}\frac{1}{2}\frac{1}{2}\}$ position for the 18% La-doped compound, showing the variation of the square of the staggered magnetization with temperature and a Neel temperature of $T_N \approx 10$ K for the Pr spins.

C. Cu spin ordering

Cu spins in Pr123 have been observed[10,31–33] to order antiferromagnetically at around 280 K. The fitted Curie-Weiss curves shown in Fig. 4 represent the contribution from paramagnetic Pr spins to χ'. If the fit is performed using data obtained between 25 and 320 K instead of between 25 and 200 K, a difference of ~5% resulted for all fitted values. This difference is mainly due to the small inflection that occurs at around 280 K, which can be readily seen in the $\chi'(T)$ measured using a stronger driving field. Shown in Figs. 7(a), 7(b), and 7(c) are the $\chi'(T)$ measured using a driving field with an rms strength of 15 Oe and a frequency of 10^3 Hz for the 9, 18, and 29 % doped compounds, respectively. These $\chi'(T)$ follow separate Curie-Weiss curves for temperatures above and below 275 K. The separation becomes clearer if a stronger driving field is used, while an applied field smears the inflection (data not shown). Fitting the data obtained between 290 and 400 K to the Curie-Weiss expression gives the solid curves shown in the high temperature data in Fig. 7, whereas the dashed curves in the low-temperature data are the same curves shown in Fig. 4. For all three compounds, the low- and high-temperature curves meet at around 275 K, which signifies the ordering of the Cu spins, as observed[10,31] in the undoped system. No obvious change on the T_N of Cu due to La doping was then observed. Both the paramagnetic Pr and paramagnetic Cu moments contribute to the Curie-Weiss curve observed above 275 K. Note that a Curie-Weiss $\chi'(T)$ is also expected for a noninteracting two-component paramagnetic system.[34,35] Treating these two components as being statistically independent[34] and using the paramagnetic parameters that were obtained at low temperatures for the Pr moment, we then obtained an effective moment of $\mu_{\text{eff}}(\text{Cu}) \approx 1.60(4)\mu_B$ for the Cu in all three compounds.

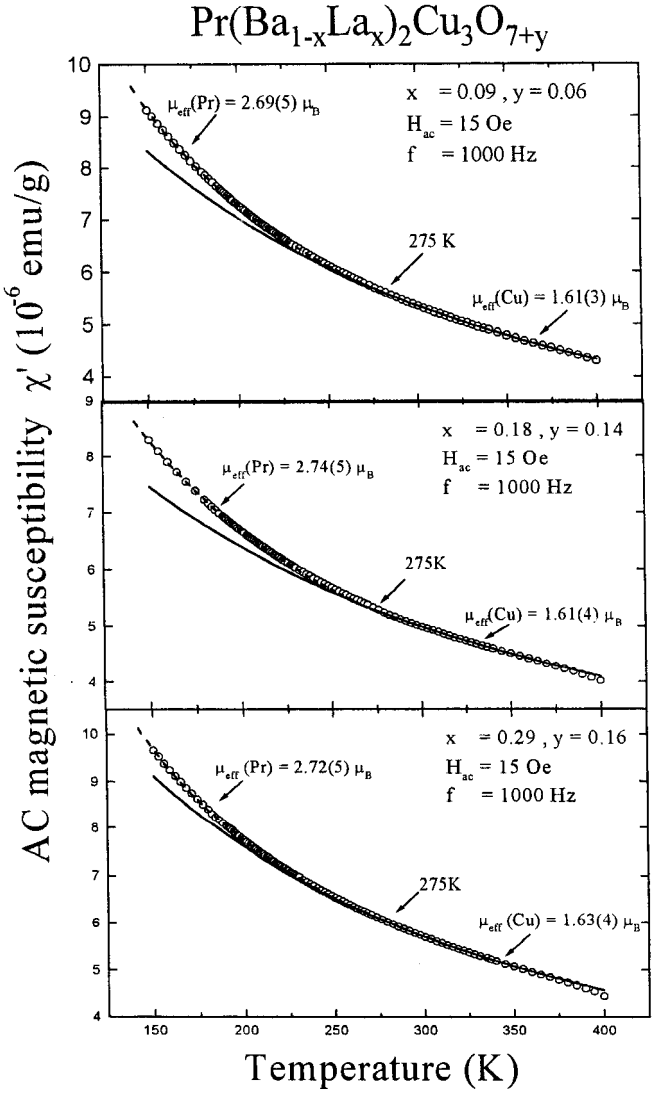

FIG. 7. Temperature dependence of the in-phase component of the ac susceptibility measured using a driving field with an rms strength of 15 Oe and a frequency of 10^3 Hz. The low- and high-temperature Curie-Weiss curves intersect at around 275 K for all three compounds.

IV. CONCLUSIONS

Variations in the structural and magnetic properties caused by partially replacing divalent Ba using trivalent La in oxygenated Pr123 compounds have been studied. In compensating for the arrival of additional charges as Ba^{2+} was replaced by La^{3+}, extra O was pulled into the antichain sites, reducing the degree of orthorhombicity in the system. A tetragonal symmetry was observed for the 29% La-doped compound. The appearance of O on the antichain sites pulled the neighboring (Ba/La)O and CuO_2 layers slightly toward the CuO_{1+y} layers, which resulted in a larger separation between the Pr and its neighboring O in the CuO_2 layers, and hence a weaker coupling between the Pr spins. Consequently, the ordering temperature of the Pr spins was significantly reduced, with a $T_N \approx 7$ K being observed for Pr spins in the 29% La-doped compound. However, the magnetic structure of Pr remains a simple antiferromagnetic arrangement. No significant structural alternations in the CuO_2 layers and no obvious changes on the T_N of Cu were found.

ACKNOWLEDGMENTS

Identification of commercial equipment in the text is not intended to imply any recommendation or endorsement by the National Institute of Standards and Technology. This work was supported by the National Science Council of the R.O.C. under Grants No. NSC 89-2112-M-008-032 (NCU) and NSC 89-2112-M-007-023 (NTHU).

[1] G. Y. Guo and W. M. Temmerman, Phys. Rev. B **41**, 6372 (1990).
[2] M. E. López-Morales, D. Ríos-Jara, J. Tagüeña, and R. Escudero, Phys. Rev. B **41**, 6655 (1990).
[3] R. Fehrenbacher and T. M. Rice, Phys. Rev. Lett. **70**, 3471 (1993).
[4] Y. Takano, S. Yokoyama, K. Kanno, and K. Sekizawa, Physica C **252**, 61 (1995).
[5] J. J. Neumeier, T. Bjornholm, M. B. Maple, and I. K. Schuller, Phys. Rev. Lett. **63**, 2516 (1989).

[6] H. B. Radousky, J. Mater. Res. **7**, 1917 (1992).
[7] Y. G. Zhao, S. Y. Xiong, Y. P. Li, B. Zhang, and S. S. Fan, Phys. Rev. B **56**, 9153 (1997).
[8] W.-H. Li, J. W. Lynn, S. Skanthakumar, and T. W. Clinton, A. Kebede, C.-S. Jee, J. E. Crow, and T. Mihalisin, Phys. Rev. B **40**, 5300 (1989).
[9] K. Nehrke and M. W. Pieper, Phys. Rev. Lett. **76**, 1936 (1996).
[10] S. Uma, W. Schnelle, E. Gmelin, G. Rangarajan, S. Skanthakumar, J. W. Lynn, R. Ealter, T. Lorenz, B. Büchner, E. Walker, and A. Erb, J. Phys.: Condens. Matter **10**, L33 (1998).
[11] H. A. Blackstead, J. D. Dow, D. B. Chrisey, J. S. Horwitz, M. A. Black, P. J. McGinn, A. E. Klunzinger, and D. B. Pulling, Phys. Rev. B **54**, 6122 (1996).
[12] Z. Zou, J. Ye, K. Oka, and Y. Nishihara, Phys. Rev. Lett. **80**, 1074 (1998).
[13] K. Takita, H. Akinaga, T. Ohshima, Y. Takeda, and M. Takano, Physica C **191**, 509 (1992).
[14] S. K. Malik, S. M. Pattalwar, C. V. Tomy, R. Prassd, N. C. Soni, and K. Adhikary, Phys. Rev. B **46**, 524 (1992).
[15] R. W. McCallum, M. J. Kramer, K. W. Dennis, M. Park, H. Wu, and R. Hofer, J. Electron. Mater. **24**, 1931 (1995).
[16] W. H. Tang and J. Gao, Physica C **315**, 66 (1999).
[17] E. Goodilin, M. Iimonov, A. Panfilov, N. Khasanova, A. Oka, S. Tajima, and Y. Shiohara, Physica C **300**, 250 (1998).
[18] M. J. Kramer, K. W. Dennis, D. Falzgraf, R. W. McCallum, S. K. Malik, and W. B. Yelon, Phys. Rev. B **56**, 5512 (1997).
[19] W.-H. Li, Y. F. Lin, S. Y. Wu, W. T. Hsieh, K. C. Lee, J. W. Lynn, C. C. Lai, and H. C. Ku, J. Appl. Phys. **79**, 6568 (1996).
[20] H. M. Rietveld, J. Crystallogr. Soc. Jpn. **2**, 65 (1969).
[21] Additional details can be found in J. W. Lynn, J. A. Gotaas, R. N. Shelton, H. E. Horng, and C. J. Glinka, Phys. Rev. B **31**, 5756 (1985).
[22] F. Beech, S. Miraglia, A. Santoro, and R. S. Roth, Phys. Rev. B **35**, 8778 (1987).
[23] A. C. Larson and R. B. Dreele, Los Alamos National Laboratory Report No. LA-UR-86-748, 1990 (unpublished).
[24] H. M. Luo, B. N. Lin, Y. H. Lin, H. C. Chiang, Y. Y. Hsu, T. I. Hsu, T. J. Lee, H. C. Ku, C. H. Lin, H.-C. I. Kao, J. B. Shi, J. C. Ho, C. H. Chang, S. R. Hwang, and W.-H. Li, Phys. Rev. B **61**, 14 825 (2000).
[25] D. B. Mitzi, P. T. Feffer, J. M. Newsaw, K. J. Webb, P. Klavins, A. J. Jacobson, and A. Kapitulnik, Phys. Rev. B **38**, 6667 (1998).
[26] B. Okai, M. Kosuge, H. Nozaki, K. Takahashi, and M. Ohta, Jpn. J. Appl. Phys. **27**, L41 (1988).
[27] L. Soderholm and G. L. Goodman, J. Solid State Chem. **81**, 121 (1989).
[28] C. C. Lai, T. J. Lee, H. K. Fun, H. C. Ku, and J. C. Ho, Phys. Rev. B **50**, 4092 (1994).
[29] M. Guillaume, P. Allenspach, W. Henggeler, J. Mesot, B. Roessli, U. Staub, P. Fischer, A. Furrert, and V. Trounov, J. Phys.: Condens. Matter **6**, 7963 (1994).
[30] M. Takata, T. Takayama, M. Sakata, S. Sasaki, K. Kodama, and M. Sato, Physica C **263**, 340 (1996).
[31] S. Skanthakumar and J. W. Lynn, Phys. Rev. B **56**, 9153 (1997).
[32] V. N. Narozhnyi, D. Eckert, K. A. Nenkov, G. Fuchs, T. G. Uvarova, and K.-H. Muller, Physica C **312**, 233 (1999).
[33] A. T. Boothroyd, A. Longmore, N. H. Andersen, E. Brecht, and T. Wolf, Phys. Rev. Lett. **78**, 130 (1996).
[34] J. S. Smart, *Effective Field Theories of Magnetism* (Saunders, London, 1966).
[35] M. Tovar, J. Appl. Phys. **83**, 7201 (1998).